

Quantifying structural damage from self-irradiation in a plutonium superconductor

C. H. Booth,¹ E. D. Bauer,² M. Daniel,¹ R. E. Wilson,^{1,*}
J. N. Mitchell,³ L. A. Morales,³ J. L. Sarrao,² and P. G. Allen⁴

¹*Chemical Sciences Division, Lawrence Berkeley National Laboratory, Berkeley, California 94720, USA*

²*Materials Physics and Applications Division, Los Alamos National Laboratory, Los Alamos, New Mexico 87545, USA*

³*Materials Science and Technology Division, Los Alamos National Laboratory, Los Alamos, New Mexico 87545, USA*

⁴*Materials Science and Technology Division, Lawrence Livermore National Laboratory, Livermore, California 94550, USA*

(Dated: August 4, 2021)

The 18.5 K superconductor PuCoGa₅ has many unusual properties, including those due to damage induced by self-irradiation. The superconducting transition temperature decreases sharply with time, suggesting a radiation-induced Frenkel defect concentration much larger than predicted by current radiation damage theories. Extended x-ray absorption fine-structure measurements demonstrate that while the local crystal structure in fresh material is well ordered, aged material is disordered much more strongly than expected from simple defects, consistent with strong disorder throughout the damage cascade region. These data highlight the potential impact of local lattice distortions relative to defects on the properties of irradiated materials and underscore the need for more atomic-resolution structural comparisons between radiation damage experiments and theory.

PACS numbers: 71.27.+a, 74.70.Tx, 61.80.-x, 61.10.Ht

I. INTRODUCTION

Plutonium is arguably the most complex and least understood of all elements, ultimately due to the propensity of its $5f$ -electrons to simultaneously reside in bonding and non-bonding electronic states. Theoretical models of δ - and α -Pu, for instance, show promise for explaining this complex behavior,^{1,2,3} but assume a homogeneous crystalline structure despite unavoidable self-irradiation damage, which can significantly alter magnetic and electronic properties. Superconductors provide a path for elucidating radiation damage effects⁴ since their properties are especially vulnerable to atomic-level structural disorder. Here, we report extended x-ray absorption fine-structure (EXAFS) measurements on the PuCoGa₅ superconductor⁵ that demonstrate the local structure of aged material is damaged at least an order of magnitude faster than theoretical predictions focusing on Frenkel defects indicate.⁶ These results explain the sharp reduction of the superconducting critical temperature, T_c , with time and underscore the need for improved radiation damage models relevant not only for understanding plutonium superconductors, but also for Pu metal and other radioactive materials.

In addition to changing fundamental properties in elemental Pu and PuCoGa₅, radiation damage affects many aspects of science and industry, for example, in semiconductors, nuclear power generation and its associated waste disposal, and the aging nuclear stockpile. Consequently, radiation damage has been studied for over a century, and intensely since World War II. Although experimental measures have provided ample verification of long-range (>10 nm) structural effects due to radiation damage, atomic-resolution descriptions of the damage induced in a crystal have relied almost exclusively on theoretical calculations. This reliance has been predictably dangerous. Recent^{7,8} nuclear magnetic reso-

nance (NMR) experiments reveal that radiation damage accumulates about 5 times faster in zircons and other ceramics than calculations indicate, calling into question both the theoretical calculations and the viability of nuclear waste containment schemes. Experimental studies have not generally kept pace with theoretical treatments of fully relaxed damage cascade structures at the atomic level. Damage cascade calculations have not been quantitatively compared to any atomic-resolution experiments until very recently,^{7,8} and never to our knowledge in intermetallics⁹ or technologically important materials such as δ -Pu. Measurements of such structural changes are vital to verify and improve these theories, and for comparison to more complex theories of dislocation loops, He bubble formation, and volume expansion.

Because large regions of a given sample remain in an undamaged state while damaged regions no longer have translational symmetry, traditional scattering techniques such as Rietveld analysis of powder diffraction data have not generated a quantitative measure of the damage fraction of a material. Local probes that treat ordered and disordered regions on an equal footing should be able to provide a more detailed, atomic-level description of the damage. NMR is one such technique, although it does not easily lend itself to a direct structural interpretation. The EXAFS technique employed here provides another local probe and has the advantage that it gives radial pair-distance distribution information around a specific atomic species, since it relies on the backscattering of a photoelectron from a core excitation.

To investigate structural radiation damage effects at the atomic level in plutonium, we employ superconducting PuCoGa₅ (Fig. 1). The unusual properties of this 18.5 K superconductor, i.e., a nearly ten-fold higher T_c than any other heavy-fermion related intermetallic and an electronic structure that bears a strong resemblance to δ -Pu, have been well characterized.^{5,10,11} Superconduct-

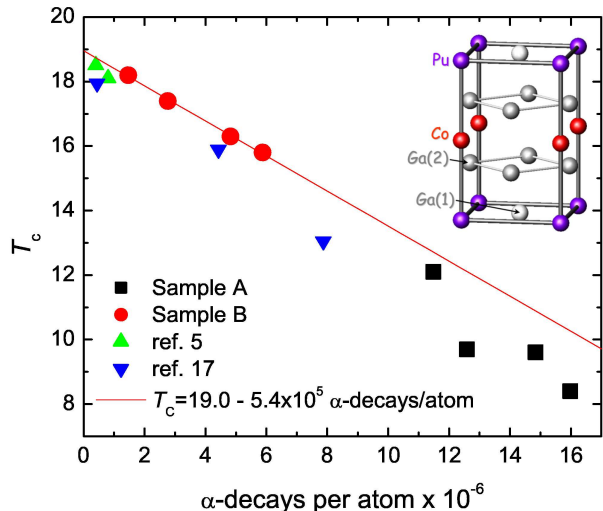


FIG. 1: (Color online) The superconducting transition temperature (T_c) as measured by magnetometry as a function of the α -decays per atom for this study (samples **A** and **B**) and in the literature (1 yr = 4.9×10^{-6} α -decays per atom for these samples). A linear decay of T_c (—) starting from about 19.0 K and decaying at a rate of about 5.4×10^5 K per α -decay per atom is also shown for reference. The inset shows the crystal structure of PuCoGa_5 .⁵

ing properties that change with time due to plutonium α -decay include a decrease in T_c by ~ 0.2 K per month (Fig. 1), the upper critical field $H_{c2} \approx 70$ T, and large critical current density $J_c > 10^4$ A/cm² for $T > 0.9T_c$,⁵ likely caused by damage-induced scattering and pinning centers. In addition, the impurity scattering rate inferred from NMR experiments follows the observed change in T_c .¹¹

Although a modern theoretical treatment of radiation damage in PuCoGa_5 is currently not available, we utilize calculations on the structurally similar δ -Pu system for comparison.⁵ In these models, the α -particle generated by the decay of a ^{239}Pu nucleus has about 5 MeV of energy and ballistically generates ~ 300 Frenkel defect pairs over a distance of nearly a micron.⁶ Most of the damage, however, is done by the recoiling ^{235}U nucleus with 86 keV, which produces ~ 2300 Frenkel pairs. A typical generated damage cascade extends over nearly 10 nm, with a defect volume fraction of about 3%. It is important to note that only the effect of Frenkel-type defects are considered in this view of radiation damage; however, these models form the basis of most modern theories such as molecular dynamics theories (for example, see Ref. 12). In fact, lattice relaxation can occur during the intermediate time-scales after these displacement events, and have been explored in various metallic systems with molecular dynamics and kinetic Monte Carlo techniques. These latter calculations show that the effective number

of defects is reduced by as much as an order of magnitude within only a few picoseconds due to additional defect migration.¹³ These values should not change substantially in PuCoGa_5 , and in fact a rough TRIM code¹⁴ calculation (which does not include the longer-time scale defect migration) using default values generates similar damage rates and ranges to the models above. We therefore expect far fewer than the initial $N_D \sim 2600$ pair defects to survive the defect migration per α -decay. Using an α -decay rate $\lambda_\alpha \approx 3.4 \times 10^{-5}$ per Pu per year from the samples discussed below, the expected upper-limit damage fraction $f_{\text{tot}} = 2N_D\lambda_\alpha/7 \approx 2.5\%$ after one year, with $1/7^{\text{th}}$ of the atoms being Pu. T_c is reduced by 50% after about 3 years (Fig. 1). These damage estimates therefore indicate that, including the expected additional defect migration, $f_{\text{tot}}(T_c/T_{c0} = 50\%) \ll 7.5\%$. This estimate is inconsistent with what one expects in a short coherence length superconductor: Within the Bogoliubov-de Gennes (BdG) formalism with strong scattering and a coherence length $\xi_0 \approx 2.1$ nm⁵, the *lower limit* (strong scattering limit) damage fraction is $f_{\text{BdG}}(T_c/T_{c0} = 50\%) \approx 15\%$.¹⁵ This value is consistent with recent studies of $\text{Ce}_{1-x}\text{La}_x\text{CoIn}_5$ ¹⁶ and $\text{CeCoIn}_{5-x}\text{Sn}_x$ ¹⁷ where the substitutions are mostly within the superconducting planes, and therefore likely produce strong scattering. The critical damage fraction should be higher when defects are randomly distributed, as with radiation damage.

This paper continues with a description of the sample characterization and other experimental methods (Sec. II), details of the data analysis and results (Sec. III), a discussion of the implications of these results (Sec. IV) and a concluding summary (Sec. V).

II. EXPERIMENTAL METHODS

Two PuCoGa_5 samples were synthesized from Ga flux.⁵ At the time of the most recent x-ray measurements, one was about 3 years old (sample **A**), and the other was about 1 year old (sample **B**). Superconducting critical temperatures were measured in a Quantum Design Magnetic Properties Measurement System as the point at which diamagnetism was observed in 10 Oe (Fig. 1). The isotopic content is the same for both samples with the main radioactivity coming from 93.93% ^{239}Pu , 5.85% ^{240}Pu , and 0.12% ^{241}Pu . The accumulated dose has been shown to be a reasonable indicator of how sample properties change with time,¹⁸ and we report the sample age in units of α -decays per atom (1 yr = 4.9×10^{-6} α -decays per atom in the formula unit). We do not use the more common “displacements per atom” (dpa) unit, because it generally assumes the number of displaced atoms (Frenkel pairs) is known from theoretical models, and we show below that this assumption may not be correct.

The material was triply contained for EXAFS experiments using epoxy- and indium-sealed kapton windows, and placed into a LHe flow cryostat at $T \leq 30$ K. Sample **A** was initially measured (measurements with

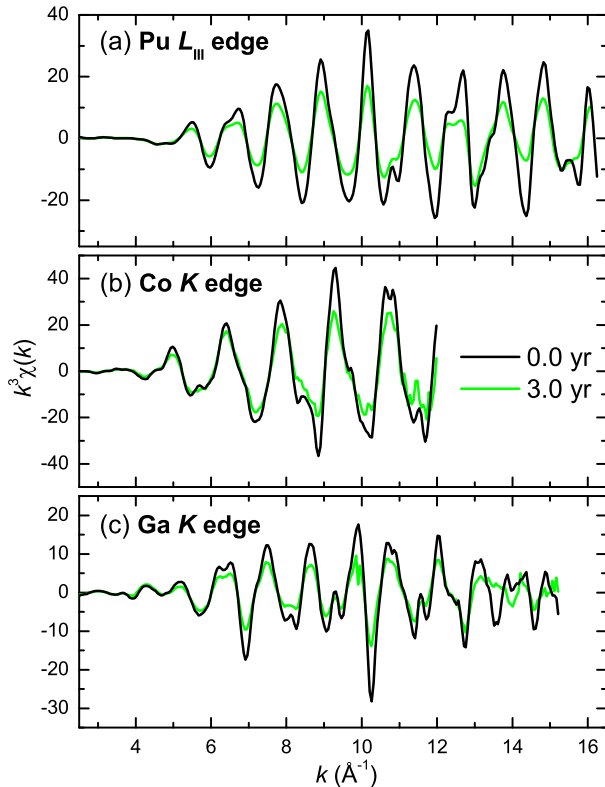


FIG. 2: (Color online) EXAFS data $k^3\chi(k)$ vs. k from the (a) Pu L_{III} edge, (b) the Co K edge, and (c) the Ga K edge, for a fresh (—, 0.2×10^{-6} α -decays per atom) and an aged (—, 14.5×10^{-6} α -decays per atom) sample.

$\leq 4 \times 10^{-6}$ α -decays per atom) as a single crystal in fluorescence mode using 30-element Ge detectors, with the data corrected for dead time and self absorption.¹⁹ Otherwise the samples were ground for the EXAFS experiments and passed through a 32 μm sieve, with about 8 mg of this powder mixed with dried boron nitride and packed into an aluminum frame. Transmission and fluorescence data agree quantitatively. This sample mass resulted in a change in absorption across the Pu L_{III} edge $\Delta\mu_a$ of ~ 0.5 absorption lengths, whereas $\Delta\mu_a \sim 0.3$ and $\Delta\mu_a \sim 2.2$ absorption lengths across the Co and Ga K edges, respectively. EXAFS spectra were collected at the Stanford Synchrotron Radiation Laboratory on beamlines 10-2 and 11-2 over a three year period, at the Pu L_{III} , Co K , and Ga K edges, generally using a half-tuned, double crystal Si(220) monochromator. The monochromator resolution was adjusted such that it was well below the core-hole lifetime at a given edge. The data were analyzed using standard procedures.²⁰ In particular, the embedded atom absorption μ_0 was determined using a cubic spline with between 4 and 6 knots over the data range, which was typically about 1 keV above the absorption threshold, E_0 , as determined by the position of

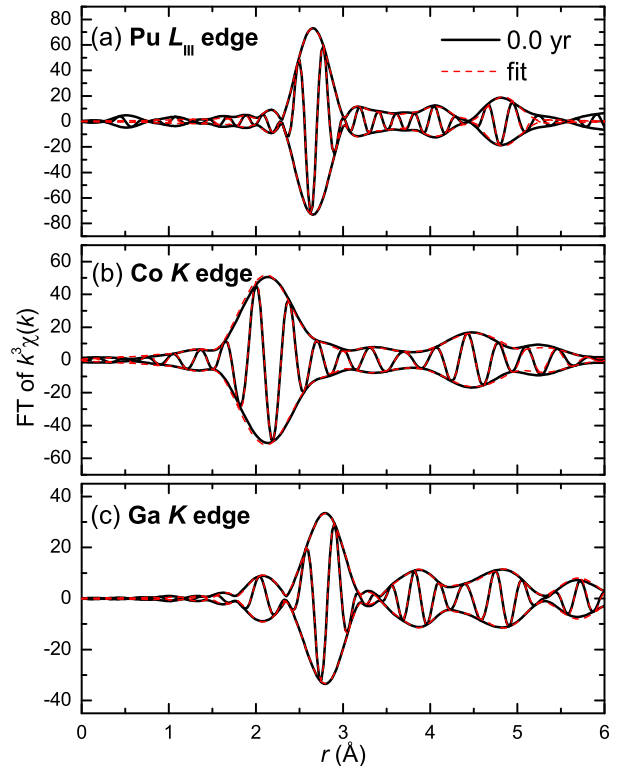


FIG. 3: (Color online) Fourier transform (FT) of the $k^3\chi(k)$ data of the fresh sample (—) in Fig. 2, together with a fit to these data (- - -). The fit quality is such that the fit is difficult to distinguish from the data. The outer envelope is \pm the transform amplitude and the inner modulating line is the real part of the complex transform. The Pu edge data (a) are transformed between 2.5-16.0 \AA^{-1} , Gaussian broadened by 0.3 \AA^{-1} , and are fit between 2.0 and 5.0 \AA . The Co edge data (a) are transformed between 2.5-11.0 \AA^{-1} , Gaussian broadened by 0.3 \AA^{-1} , and are fit between 2.0 and 5.5 \AA . The Ga edge data (a) are transformed between 2.5-15.0 \AA^{-1} , Gaussian broadened by 0.3 \AA^{-1} , and are fit between 1.6 and 5.0 \AA .

the half-height of the absorption change at the edge. The data were fit in r -space using the RSXAP package²¹ with theoretical scattering functions generated by FEFF7.²²

III. ANALYSIS AND RESULTS

Figure 2 shows an example of the normalized oscillations in the absorption above each measured edge as a function of k , the photoelectron wave vector, for the fresh (0.2×10^{-6} α -decays per atom) and 3 year old (14.5×10^{-6} α -decays per atom) samples. A Fourier transform (FT) of such data (Fig. 3) produces peaks in the amplitude as a function of the distance r from the absorbing atomic species corresponding to neighboring atoms. For instance, the dominant peak in the Pu edge

TABLE I: EXAFS fit results for the Pu L_{III} and the Co K edges on a fresh (0.2×10^{-6} α -decays per atom) sample of PuCoGa₅. Fit and transform ranges are listed in Fig. 3. All single-scattering peaks within the fit range are included in these fits. Multiple scattering was only included in the Ga edge fits to avoid errors originating from peak overlap, but the results from these scattering paths are in themselves unreliable and so are not reported. Coordination numbers, N , are held fixed to the nominal structure. S_0^2 , ΔE_0 , and $R(\%)$ are 0.89(5), -4.7(3) eV and 3.6% for the Pu edge, 0.85(5), 5(1) eV, and 6.1% for the Co edge, and 0.85(3), -1.7(4), and 6.9% for the Ga edge, respectively. The number of free parameters in the fits are 10, 14, and 15 for the Pu, Co, and Ga edges, respectively, and are far below the number of independent data points as given by Stern's rule.²³ The quoted error on each quantity is the greater of that obtained by comparisons to standard materials,²⁰ repeated measurements, and a Monte-Carlo method.²⁴ The nature of the Ga local environment required constraints on several parameters to obtain meaningful fits, as indicated. Constraints on the pair distances in the Ga edge fits assume a tetragonal 115 structure such that Ga(1) sits at the center of the Pu ab face and a plane of Co atoms splits a plane of Ga(2).

	N	σ^2 (\AA^2)	R (\AA)	R_{diff}^5 (\AA)	Θ_{cD} (K)	σ_{stat}^2 (\AA^2)
Pu-Ga(1)/Ga(2)	12	0.00174(9)	2.97(1)	2.993	330(20)	-0.0001(2)
Pu-Co	2	0.0019(4)	3.38(2)	3.393	420(30)	0.0002(2)
Pu-Pu	4	0.0016(2)	4.21(2)	4.232	270(20)	0.0004(2)
Pu-Ga(2)	24	0.0038(4)	5.16(3)	5.165	270(20)	0.0012(4)
Co-Ga(2)	8	0.0019(1)	2.45(1)	2.471	250(20)	0.0004(2)
Co-Pu	2	0.005(3)	3.38(5)	3.393		
Co-Co	4	0.007(7)	4.18(8)	4.232		
Co-Ga(1)	8	0.006(1)	4.5(1)	4.524		
Co-Ga(2)	16	0.0030(6)	4.84(2)	4.901		
Ga(1)-Pu	4	0.0022(2) ^a	2.97(1) ^{bg}	2.993		
Ga(1)-Ga(2)	8	0.0053(2) ^c	2.95(1) ^d	2.993		
Ga(1)-Ga(1)	8	0.0051(2) ^e	4.20(2) ^{fgh}	4.232		
Ga(1)-Co	8	0.0023(5)	4.51(1)	4.524		
Ga(2)-Co	2	0.017(2)	2.43(1) ^h	2.471		
Ga(2)-Ga(2)	1	0.0026(2)	2.45(1) ^h	2.552		
Ga(2)-Ga(2)	4	0.0053(2) ^c	2.97(1) ^b	2.993		
Ga(2)-Ga(1)	2	0.0053(2) ^c	2.95(1) ^d	2.993		
Ga(2)-Pu	8	0.0022(2) ^a	2.95(1) ^d	2.993		
Ga(2)-Ga(2)	4	0.0051(2) ^e	3.94(2)	3.933		
Ga(2)-Ga(2)	5	0.0051(2) ^e	4.20(2) ^f	4.232		

^{a-f}like symbols held equal

$${}^g r_{\text{Ga}(1)\text{-Ga}(1)} = \sqrt{2} r_{\text{Ga}(1)\text{-Pu}}$$

$${}^h r_{\text{Ga}(2)\text{-Ga}(2)} = \sqrt{4r_{\text{Ga}(2)\text{-Co}}^2 - r_{\text{Ga}(1)\text{-Ga}(1)}^2}$$

data (Fig. 3a) corresponds to the 12 Pu-Ga neighbors at ~ 3.0 \AA . Note that the atomic scattering functions generate complicated lineshapes, causing shifts in the peak positions from the actual structure that are well reproduced by calculations using FEFF7.²² Information about the local structure is therefore obtained by fitting these calculated scattering functions to these data. The results of fits to data from fresh material that has not undergone a significant amount of α -decay are reported in Fig. 3 and Table I. The fit quality is excellent, and all the measured pair distances agree well with diffraction results. We note that the local environment around Ga is more complicated than around Pu or Co, and therefore constraints were necessary to reduce the number of fit parameters while still obtaining high quality fits. Unfortunately, constraints add an unknown amount of systematic error that is not reflected in the estimated errors, and we ascribe discrepancies between diffraction and EXAFS results from the Ga K -edge data to this source. Where

the data are of sufficient quality, the temperature dependence of the mean-squared displacements of the pair distances, σ^2 's, were obtained and are well described by a correlated-Debye model²⁵ with reasonable values of the correlated-Debye temperatures, Θ_{cD} 's, (for comparison to δ -Pu, see Ref. 26), and no evidence of static disorder from the fitted offsets, σ_{stat}^2 's.

Significant radiation damage effects are readily apparent in the raw data with a marked decrease in the overall amplitude of the spectra as samples are aged up to 3 years (Fig. 4). Preliminary fits to the data from the aged samples showed that the decrease in amplitude in the data is due both to a decrease in the overall scale factor S_0^2 and an increase in each atom pair's σ^2 with age. This situation indicates that there are at least three distinct regions within the aged samples: virtually undamaged, strongly damaged where the distance widths σ_s^2 are large enough that the local structure no longer contributes to the EXAFS amplitude, and mildly damaged where the σ_m^2 's only

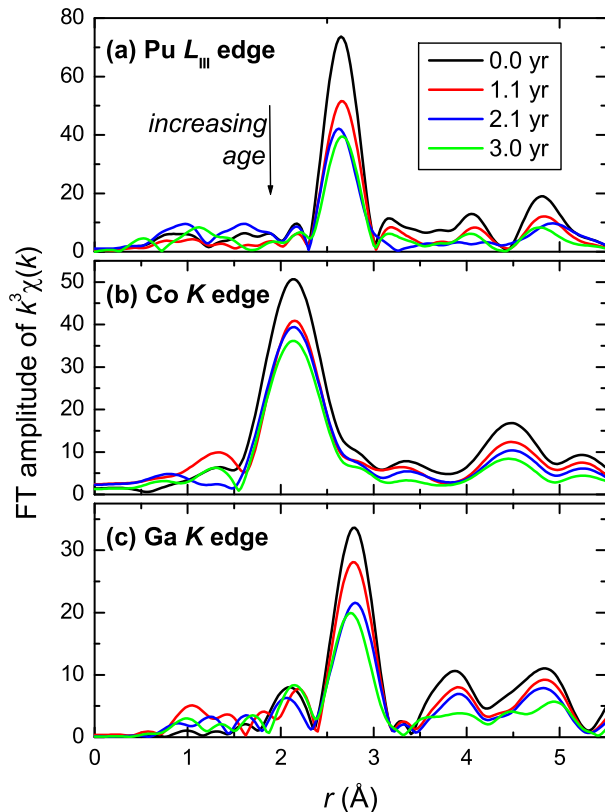


FIG. 4: (Color online) FT of the $k^3\chi(k)$ EXAFS data from the (a) Pu L_{III} , (b) Co K , and the (c) Ga K edges are shown for sample ages about one year apart. Samples have accumulated doses of 0.2×10^{-6} α -decays per atom (—), 5.4×10^{-6} α -decays per atom (—), 10.2×10^{-6} α -decays per atom (—), and 14.5×10^{-6} α -decays per atom (—). Transform ranges are between 2.5–16.0 \AA^{-1} , 2.5–10.0 \AA^{-1} , and 2.5–14.5 \AA^{-1} , respectively, all Gaussians broadened by 0.3 \AA^{-1} .

allow for a weak contribution. The latter regions may exist, for instance, on the edges of strongly damaged regions. We therefore describe f_{tot} as due to the sum of the strongly damaged fraction f_s and the mildly damaged fraction f_m . Since EXAFS amplitudes $A \sim 1/\sigma$, as long as σ_m is large enough, $f_{\text{tot}} \approx 1 - S_0^2(t)/S_0^2(0)$, where $S_0^2(t)$ is obtained from fits where $\sigma^2(t)$ are fixed at $\sigma^2(0)$. That is, the total damage fraction in aged samples can be estimated by fixing most fitting parameters to those obtained from fresh-sample fits, and estimating f_{tot} by the change in amplitude as given by S_0^2 . These damage fractions are shown in Fig. 5 and demonstrate strong damage production at apparently different rates for each atomic species.

Using this estimate of f_{tot} , f_s is approximated by performing a fit where the $\sigma^2(t)$'s are no longer constrained, in which case $f_s \approx (S_0^2(t) - S_0^2(t))/S_0^2(0)$. Correlations between the S_0^2 and σ^2 parameters are more difficult to control in such a procedure, but fits to Pu edge data in-

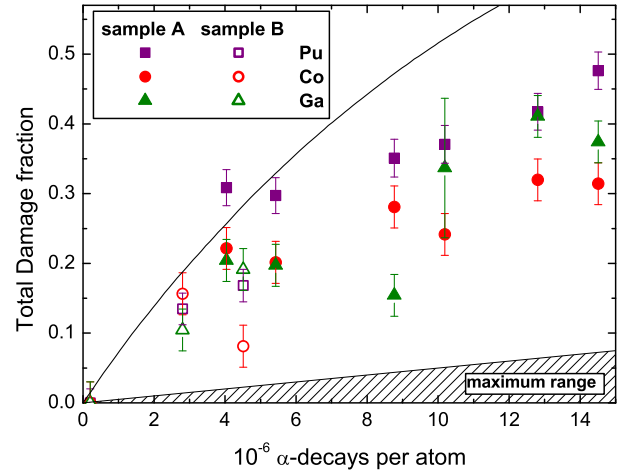


FIG. 5: (Color online) The total fraction of displaced atoms as a function of the number of α -decays per atom, as seen from each atomic species. Error bars are based on reproducibility. Absolute errors are about $\pm 5\%$. The line shows percolation behavior based on the first two aged Pu data points for sample A, and the hashed area gives the theoretical range of damage up to the amount expected in the absence of defect migration.

indicate that between 60–80% of the damage is due to the strongly damaged regions and σ_m is enhanced by ~ 0.010 – 0.015\AA^2 over the well-ordered regions for all of the aged samples measured. Similar results are obtained from the Co and Ga edge data.

IV. DISCUSSION

The accumulated damage after one year in sample A is measured as between 20–30% from the point of view of each of the constituent atoms in PuCoGa_5 . This value is an order of magnitude higher than theoretical estimates that only account for defects, or closer to two orders of magnitude if one allows for defect migration after defect formation.¹³ It is important to note at this point that the damage enhancement, while possibly indicating more defects than expected, may also indicate significantly more defect-induced lattice strain and distortions. In fact, this amount of damage is so large that, assuming a ~ 10 nm damage cascade as expected for δ -Pu, *every* atom in the cascade is displaced from its equilibrium position. Modern molecular dynamics calculations should, in principle, generate significant lattice distortions around defects induced by radiation damage, but this effect has not, to our knowledge, been reported in the literature for intermetallics. In addition, the observed damage does not proceed at as fast a rate as extrapolated from lower accumulated doses. This disagreement is very likely due to self-annealing²⁷ caused by the room-temperature storage of the samples between measurements. Self-annealing is

also likely the cause of the differences between the samples (sample **B** appears to be damaging at a somewhat slower rate), as the exact history of the storage conditions for each sample then becomes important. In addition, differences between the constituent atomic species indicate different defect production or migration rates. These issues should be studied in other materials to further explore the role of self-annealing and atomic-species effects.

Another way of describing radiation damage is to consider that a decay event generates enough heat within the damage cascade that the material locally melts and then rapidly resolidifies, thus quenching disorder into the cascade region from the high temperature state and potentially also creating a distribution of competing structural phases. This picture is similar to the “thermal spike” model as originally proposed by Seitz,²⁸ although it proved to be computationally intractable.²⁹ Applying molecular dynamics after (or during) Frenkel defect production seems to combine the relevant aspects of these two schemes, and could, in principle, generate the sort of distortions measured here in PuCoGa₅. Simulated EXAFS data could be calculated from the results of future molecular dynamics calculations on PuCoGa₅ for a direct comparison of the efficacy of such models.

These data largely explain the fast reduction of T_c in PuCoGa₅, with $T_c/T_{c0} \approx 50\%$ when $f_{\text{tot}} \approx 40\%$. This value is now greater than the lower-limit damage fraction of $f_{\text{BdG}}(T_c/T_{c0} = 50\%) \approx 15\%$,¹⁵ as expected since not all damaged regions will create strong scattering. In addition, it is likely that defects outside the superconducting planes scatter more weakly than defects on the in-plane sites.^{16,17} Decreasing the effective scattering strength would increase the necessary impurity densities in the theory.

Also shown in Fig. 5 is the prediction of a cubic percolation model. The time axis is chosen such that the model agrees with the first aged Pu edge data points for sample **A**. Because of the strong damage that occurs within a cascade, the superconducting fraction is likely more closely related to the fraction of the material that exists within the volume between the edges of damage cascades, which is better described by the percolation model depicted in Fig. 5. According to this extrapolation one might expect superconductivity to cease between 3.5 and 4 years for these samples ($f_{\text{tot}} \sim 0.8$), roughly consistent with the data in Fig. 1, although no samples have yet been observed to become non-superconducting at this time. This simplification, of course, doesn’t account for any proximity effects, which should increase this time period, or any increased impurity scattering, which would decrease this time.

The emerging physical picture of PuCoGa₅ is one where the recoiling U nucleus generates much more damage than expected based on models of elemental Pu. This damage is likely dominated by near-neighbor lattice distortions that extend into the second coordination sphere or beyond, possibly generating local distributions of im-

purity phases. This damage is so severe that it encompasses all the atoms in a given damage cascade. The effective damage rate is slowed as the material anneals at room temperature. Photoemission results indicate that the $5f$ electrons have both local and itinerant character in PuCoGa₅.¹⁰ The partially localized f electrons in the well-ordered material are likely further localized in the damaged regions, in analogy to δ -Pu.³⁰ This view is consistent with x-ray absorption near-edge measurements on aged PuCoGa₅ samples.³¹ Radiation damage therefore probably creates non-superconducting material both due to enhanced localization and strong defect scattering in these regions, although a proximity effect could still allow some superconductivity. Annealed areas within a damage cascade probably would not be superconducting due to their limited size, unless they reach the edge of a cascade.

These data support and extend the conclusion of Farnan *et al.*^{7,8} that radiation damage occurs at a much faster rate than current theoretical predictions. In their work, the measured damage production rate is about 5 times higher than the theoretical prediction for the unrelaxed defect production rate in zircons. In the present work, we find a production rate at least 10 times faster than the prediction in an intermetallic, and observe deviations from a percolation model that we ascribe to annealing effects. The role of annealing should be carefully considered in studies of zircons and related potential nuclear-waste storage materials.

V. CONCLUSION

Local structure data on samples of PuCoGa₅ demonstrate a well-ordered local lattice structure that agrees with the long-range average structure obtained by diffraction measurements. After the sample has aged long enough to accumulate a significant total number of α -decays, the local structure exhibits strong disorder, primarily through a reduction in the amplitude of the EXAFS oscillations, but also in the pair-distance distribution variances σ^2 's. This disorder affects between 20-30% of sample **A** after one year ($\sim 4 \times 10^{-6}$ α -decays per atom), followed by a somewhat slower damage accumulation rate. Theoretical estimates that only account for defects predict at least an order of magnitude less damage, not including the damage-reducing factors of self-annealing and defect migration. These data help explain the fast reduction of the superconducting transition temperature both in terms of defect scattering and a simple percolation model.

These results underscore the need for more local structure studies of radiation damage in general and especially in PuCoGa₅. Only through better theoretical models and atomic-level probes can we understand the detailed electronic and structural properties of damaged regions and how they couple to superconductivity. In particular, direct comparisons between damage cascade structures and

local structure measurements should be pursued. Such studies will have ramifications not only for understanding superconductivity in PuCoGa₅, but also the unusual properties of δ -Pu, and the field of radiation damage in general.

Acknowledgments

We thank M. Fluss, M. Graf, A. Kubota, L. Soderholm, J. Thompson and W. Wolfer for enlightening dis-

cussions and W.-J. Hu for assistance in loading one of the plutonium samples. Supported by the U.S. Department of Energy (DOE) under Contract No. DE-AC02-05CH11231. X-ray absorption data were collected at the Stanford Synchrotron Radiation Laboratory, a national user facility operated by Stanford University on behalf of the DOE/OBES. Work at Los Alamos was performed under the auspices of the U. S. DOE.

-
- * Permanent address: Chemistry Division, Argonne National Laboratory, 9700 South Cass Avenue, Argonne, IL 60439-4831, USA
- ¹ J. H. Shim, K. Haule, and G. Kotliar, *Nature* **446**, 513 (2007).
 - ² X. Dai, S. Y. Savrasov, G. Kotliar, A. Migliori, H. Ledbetter, and E. Abrahams, *Science* **300**, 953 (2003).
 - ³ S. Y. Savrasov, G. Kotliar, and E. Abrahams, *Nature* **410**, 793 (2001).
 - ⁴ A. R. Sweedler, C. L. Snead, and D. E. Cox, in *Treatise on Materials Science and Technology*, edited by T. Luhman and D. Dew-Hughes (Academic Press, New York, 1979), vol. 46, pp. 349–426.
 - ⁵ J. L. Sarrao, L. A. Morales, J. D. Thompson, B. L. Scott, G. R. Stewart, F. Wastin, J. Rebizant, P. Boulet, E. Colineau, and G. H. Lander, *Nature* **420**, 297 (2002).
 - ⁶ W. G. Wolfer, *Los Alamos Sci.* **26**, 274 (2000), and references therein.
 - ⁷ I. Farnan, H. Cho, and W. J. Weber, *Nature* **445**, 190 (2007).
 - ⁸ I. Farnan and E. K. H. Salje, *J. Appl. Phys.* **89**, 2084 (2001).
 - ⁹ R. S. Averback, R. Benedek, and K. L. Merkle, *Phys. Rev. B* **18**, 4156 (1978), these authors model electrical resistivity with a defect model.
 - ¹⁰ J. J. Joyce, J. M. Wills, T. Durakiewicz, M. T. Butterfield, E. Guziewicz, J. L. Sarrao, L. A. Morales, A. J. Arko, and O. Eriksson, *Phys. Rev. Lett.* **91**, 176401 (2003).
 - ¹¹ N. J. Curro, T. Caldwell, E. D. Bauer, L. A. Morales, M. J. Graf, Y. Bang, A. V. Balatsky, J. D. Thompson, and J. L. Sarrao, *Nature (London)* **434**, 622 (2005).
 - ¹² S. M. Valone, M. I. Baskes, M. Stan, T. E. Mitchell, A. C. Lawson, and K. E. Sickafus, *J. Nucl. Mat.* **324**, 41 (2004).
 - ¹³ T. D. de la Rubia, M. J. Caturla, E. A. Alonso, N. Soneda, and M. D. Johnson, *Radiation Effects and Defects in Solids* **148**, 95 (1999).
 - ¹⁴ <http://www.srim.org/>.
 - ¹⁵ M. Franz, C. Kallin, A. J. Berlinsky, and M. I. Salkola, *Phys. Rev. B* **56**, 7882 (1997).
 - ¹⁶ C. Petrovic, S. L. Bud'ko, V. G. Kogan, and P. C. Canfield, *Phys. Rev. B* **66**, 054534 (2002).
 - ¹⁷ M. Daniel, E. D. Bauer, S.-W. Han, C. H. Booth, A. L. Cornelius, P. G. Pagliuso, and J. L. Sarrao, *Phys. Rev. Lett.* **95**, 016406 (2005).
 - ¹⁸ F. Jutier, J.-C. Griveau, E. Colineau, J. Rebizant, P. Boulet, F. Wastin, and E. Simoni, *Physica B* **359-361**, 1078 (2005).
 - ¹⁹ C. H. Booth and F. Bridges, *Physica Scripta* **T115**, 202 (2005).
 - ²⁰ G. G. Li, F. Bridges, and C. H. Booth, *Phys. Rev. B* **52**, 6332 (1995).
 - ²¹ <http://lise.lbl.gov/R SXAP/>.
 - ²² A. L. Ankudinov and J. J. Rehr, *Phys. Rev. B* **56**, R1712 (1997).
 - ²³ E. A. Stern, M. Qian, Y. Yacoby, S. M. Heald, and H. Maeda, *Physica C* **209**, 331 (1993).
 - ²⁴ J. M. Lawrence, P. S. Riseborough, C. H. Booth, J. L. Sarrao, J. D. Thompson, and R. Osborn, *Phys. Rev B* **63**, 054427 (2001).
 - ²⁵ G. Beni and P. M. Platzman, *Phys. Rev. B* **14**, 1514 (1976).
 - ²⁶ E. J. Nelson, K. J. M. Blobaum, M. A. Wall, P. G. Allen, A. J. Schwartz, and C. H. Booth, *Phys. Rev. B* **67**, 224206 (2003).
 - ²⁷ M. J. Fluss, B. D. Wirth, M. Wall, T. E. Felter, M. J. Caturla, A. Kubota, and T. D. de la Rubia, *J. Alloys Compd.* **368**, 62 (2004).
 - ²⁸ F. Seitz, *Disc. Faraday Soc.* **5**, 271 (1949).
 - ²⁹ G. H. Kinchin and R. S. Pease, *Rep. Prog. Phys.* **18**, 1 (1955).
 - ³⁰ S. K. McCall, M. J. Fluss, B. W. Chung, M. W. McElfresh, D. D. Jackson, and G. F. Chapline, *Proc. Natl. Acad. Sci. U.S.A.* **103**, 17179 (2006).
 - ³¹ C. H. Booth, M. Daniel, R. E. Wilson, E. D. Bauer, J. N. Mitchell, N. O. Moreno, L. A. Morales, J. L. Sarrao, and P. G. Allen, *J. Alloys and Compds.* (in press, doi:10.1016/j.jallcom.2006.09.135.).